Journal Reprints

The British Institute of Non-Destructive Testing
1 Spencer Parade, Northampton. NN1 5AA, England
Telephone: Northampton (01604) 630124 Fax: (01604) 231489

 DOI: 10.1784/insi.2008.50.1.19

High-speed CT imaging for today's industry

D Schneberk and N Shashishekhar

Submitted 14 March 2007
Accepted 17 May 2007

Computed Tomography (CT) has been extensively used in industrial inspection, however, production applications have been few, due to the time required for performing CT. This paper describes a high-throughput, production X-ray CT system for inspecting munitions. Various types of defects such as cracks, voids, fuse armed status, and powder fill level are identified and evaluated. Automatic defect recognition algorithms and software have been developed to inspect the CT data, due to the large amount of data involved, and high throughput required.

Introduction

Computed tomography (CT) is a non-destructive evaluation technique for visualising and inspecting the internal structure of objects. The output of the CT data acquisition and reconstruction process is the 2D or 3D volumetric X-ray attenuation distribution of the object. As a by-product of the data acquisition process, the complete set of digital radiographic images of the object are obtained which can be used for further inspection and analysis.

In industry, CT has been traditionally used in non-production settings such as rocket motor inspection[1], turbine-blade inspection[2], engine-head inspection[3], reverse engineering[4], and casting process optimisation[5]. CT data acquisition and image reconstruction are time-intensive processes that have limited its use in a production environment. This paper presents a CT system designed and developed for high-throughput inspection of 40 mm cartridges. Since a large amount of data is generated with CT, to sustain high-throughput it becomes necessary to implement automatic defect recognition techniques for detecting defects.

The organisation of the paper is as follows: Section 2 outlines the inspection requirements; Section 3 gives an overview of the system components; Sections 4, 5, 6 and 7 describe each of the components in detail; and finally, conclusions are presented in Section 8.

Inspection requirements

A radiographic image of a 40 mm cartridge is shown in Figure 1. There are primarily three regions that are inspected for defects: fuse, primer cup, and *boat-tail* end.

The inspection system requirements for the cartridge are:

- Primer cup inspection for presence of powder: determined by operator from radiographic images.
- Fuse region inspection for *armed* status: determined by operator from CT slice at predefined location.
- *Boat-tail* end inspection for cracks, pores and through holes: determined by automatic defect recognition from many CT slices. The size of the smallest defect to be found is 0.25 mm over the entire contour of the *boat-tail* end, in the 0.5 mm thickness from the exterior to the middle of the cartridge.
- Inspection throughput: minimum of 60 cartridges fully classified in one hour.
- Long duty cycle capability with up-times between 16 and 22 hours.

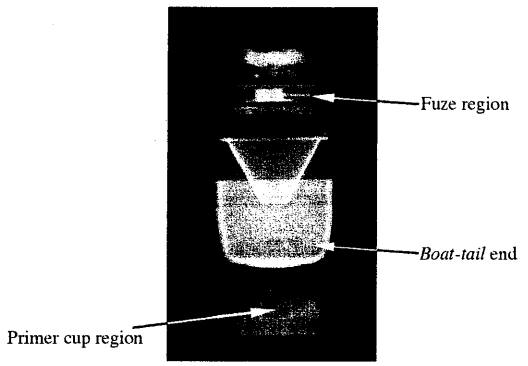

Figure 1. Radiographic image of 40 mm cartridge

System components

The CT inspection system designed and manufactured for meeting the above inspection requirements is shown in Figure 2. The main functional components of the system are shown in Figure 3. They are (i) Part handling, (ii) DR/CT scanning, (iii) CT processing and ADR, and (iv) Viewing, image archival and retrieval. In operational sequence, 40 mm cartridges are loaded into a twelve part cassette, the cassette is presented to the X-rays, each of the 40 mm cartridges is rotated independently acquiring a data set for 3D reconstruction, 3D images are then reconstructed for the separate cartridges, and using a combination of operator and automated inspection, the parts are classified and archived. The entire operation of scanning and classifying the twelve 40 mm cartridges is completed in 12 minutes, satisfying the 60 cartridges per hour requirement. Behind the different components and functions is a distributed network of computer resources configured for the different inspection tasks. To assess system performance, scanning is regularly *salted* with munitions standards with known defects.

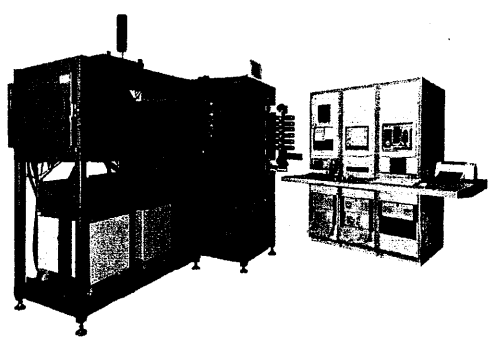

Figure 2. CT inspection system

D Schneberk and N Shashishekhar are with V J Technologies, Inc, 89 Carlough Road, Bohemia, NY 11716, USA.

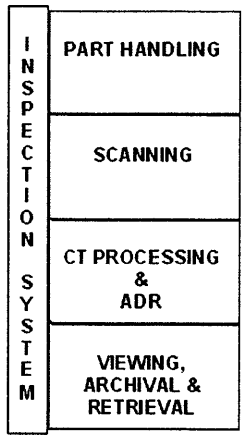

Figure 3. System functional components

Part handling

The part handling component function comprises loading/unloading, part motion for scanning, and verification of all safety and cabinet X-ray interlocks. Qualified handlers load the 40 mm cartridges into six separate multi-part holders, which are connected together to form the loaded cassette. Each part holder can accommodate two 40 mm cartridges. The cassette can hold up to twelve 40 mm cartridges in a configuration that enables them to be rotated independently in front of a large area X-ray detector. Once loaded, the cassette travels into the X-ray cabinet for DR/CT scanning. After scanning, the cassette retracts from the cabinet and handlers unload the cartridges.

Each holder is equipped with classification sensors that have a green light on if the 40 mm cartridge is verified to have acceptable fuse/primer status, and acceptable integrity in the *boat-tail* end of the munition. A red light on the individual 40 mm cartridge holder indicates an unacceptable fuse/primer status, or unacceptable *boat-tail* end integrity. At the conclusion of the unloading operation the classifying sensors reset to all lights off.

The cassette is connected to a motion control and data acquisition computer, configured to acquire the digital radiographic images for the fuse/primer inspection, and CT image reconstruction. The different high-level functions for the motion control and data acquisition computer are initiated electronically depending on the state of the cassette: data acquisition, cassette unloading, or in-transit.

Scanning

The scanning component consists of a 320-kVp X-ray tube, a large area Am-Si detector (14-bit, 0.127 mm pixel size), and an appropriate X-ray cabinet. The imaging geometry results in an overall X-ray magnification of ~1. Contrast resolution is of the order of 2%-3%. Prior to data acquisition with the cassette in place, a reference image (I0) is acquired for use in CT pre-processing. For scanning, the cassette travels to a particular position in the path of the X-ray beam-detector envelope. Position sensors indicate when the cassette is in the correct location for scanning. Once in position, the X-ray source is activated and digital radiographs of the cartridges are acquired. Up to 90 digital radiographs are acquired, and each multi-part holder is independently rotated for each acquired view from the Am-Si detector.

Once each digital radiographic view is acquired, the radiographs for the individual 40 mm cartridges are extracted from the acquired image. At selected views, the extracted images of the individual 40 mm cartridges are sent to the viewing station for primer cup inspection. Also, for every view, all the extracted images are sent to the CT processing and ADR component. Processing for CT commences immediately after the acquisition of each view, on different computing resources available within the distributed network of computers. This combination of multi-computer and data pipelining techniques speeds up the CT processing, resulting in an overall higher throughput.

Figure 4. Scanning component showing area detector and part cassette

CT processing and ADR

The entire CT processing and ADR component is built around a set of four Pentium 4 computers. The task of each computer is to process and reconstruct 3D CT data for three 40 mm cartridges. After reconstructing the 3D volume of the cartridge, Automatic Defect Recognition (ADR) techniques are applied to identify and evaluate cracks and voids in the *boat-tail* end.

In the CT processing step, digital radiographs are converted into attenuation radiographs, beam hardening corrections are applied, balanced for detector offsets and reconstructed with centre-offset, cone-beam Feldkamp[6] reconstruction algorithms. In standard rotation-only CT scanning for area detectors, alignment procedures are usually applied until the centre of the rotational table, the centre of the beam, and the centre of the area detector are on the same line. For the 40 mm cartridges in the cassette, this condition is intentionally not satisfied for any of the cartridges in the multi-part holders. Instead, *mid-line offset*[7] corrections are mapped to the different distances from the centre of the beam, which is positioned at the centre of the Am-Si detector. All of the 40 mm cartridges are reconstructed with a different set of horizontal and vertical mid-line offset corrections.

The output of the CT processing step is the complete 3D volumetric data of the cartridge. The 3D volume consists of 573 slices, each slice of size 272×272 pixels. For fuse inspection, a selected CT slice (at a predetermined location) from the 3D volume is sent to the viewing station for operator verification of fuse status. Sample CT slices for three different cartridges are shown in Figure 5, illustrating fuse armed status (reject), fuse partially armed status (reject) and fuse unarmed status (accept).

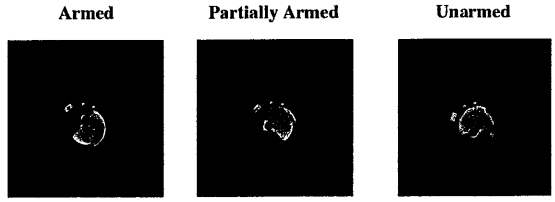

Figure 5. CT Slices of three different cartridges showing possible fuse configurations

For automated analysis of the *boat-tail* end, histogram-based thresholding and surface fitting techniques are used to extract two 2D images – the first corresponding to the bottom of the *boat-tail* end (*dome* image), and the second corresponding to the 'unfolded' side-walls of the *boat-tail* end (*circ* image). Morphological image processing algorithms are then applied to these 2D images to identify the defect pixels in the *boat-tail end*. After defect detection, the cartridge is evaluated for acceptance from defined accept/reject criteria based on the size and depth of the defects. Sample *circ* and *dome* images for three different cartridges are shown in Figure 6, with defects clearly discernible. It can be noticed that there are faint ring-like artifacts present in the dome images. Sinogram-based ring-removal algorithms applied during the CT processing step significantly attenuate these artifacts, but do not fully eliminate them. Observation of these artifacts over a population of images found them to not affect the automated analysis.

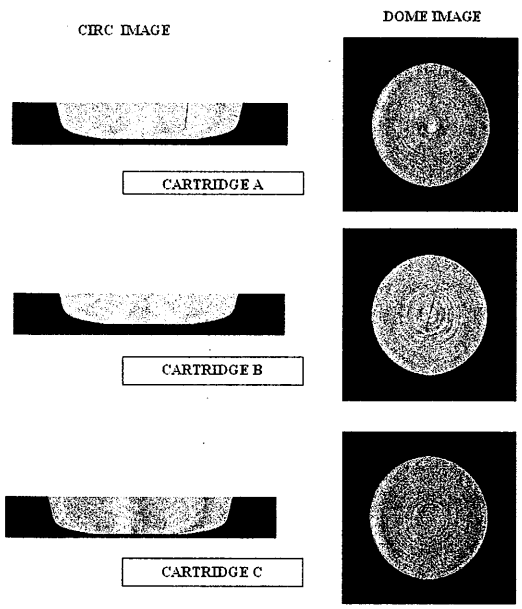

Figure 6. Circ and dome images for three different cartridges showing defects

Viewing, archival and retrieval

The viewing, archival and retrieval component has three functions: radiographic images and CT slice display for operator inspection; image and inspection record archival; and image retrieval for review and analysis. A high-performance PC with large disk capacity, equipped with a DVD-writer is used to implement this component. The viewing software displays the radiographic images (as a movie), and the appropriate CT slice of each cartridge, to enable the operator to inspect for powder fill and fuse status respectively.

A number of data objects are generated during the course of scanning for the 40 mm cartridges. For all scanned parts the digital radiographs and CT slice used in the primer/fuse inspection, and the two 2D sheets of material for the *boat-tail* end used for automated inspection, can be archived and stored on removable media. In addition, the classification of the part, and the quantitative measures that justify the particular classification, can be archived and stored. The 3D reconstructed cubes constitute a large amount of data, and contain information on many aspects of the 40 mm cartridge, not simply the *boat-tail* end. All of the data of the cartridge may be retained: digital radiographs, 2D sheets of material, classification information, and the full 3D reconstructed image. The viewing software also enables archived data retrieval, review and analysis (with possibly different parameter settings).

Conclusions

Results of the first series of scanning show good ADR performance: greater than 90% Probability of Detection (POD) and low Probability of False Alarms (PFA). Defects in the *boat-tail* end are imaged clearly and automatically detected. Equally important, this system provides inspections of the boat end, the fuse region, and the primer cup at the one minute per bullet rate. The distributed and data pipelined processing system implemented here enables a quick turnaround time in spite of the large number of calculations to be performed.

Improvements in signal-to-noise are needed to improve ADR performance. Preliminary trials show benefits to more source energy, and possibly to a change to a two-arm manipulator. More source energy would also enable faster data acquisition, and increase throughput.

In conclusion, multi-component CT with ADR can produce complete, high quality inspections of munitions within a tight time constraint. This promising approach holds many possibilities for other types of production inspection applications. Improvements in detector technology and computer speeds, already available since the time the scanner was fielded, will only make this system faster.

Acknowledgements

The authors would like to thank all project team members for their contributions, including: Vrindesh Shetty, Boris Soyfer, Steve Halliwell, Daniel Veselitza, Mario Nguyen, Michele Bergmann and Vijay Alreja.

References

1. J E Youngberg and P Burstein, 'Three dimensional computed tomography for rocket motor inspection', Proc. SPIE Nondestructive Evaluation of Aging Aircraft, Airports, Aerospace Hardware, and Materials, Vol 2455, pp 291-298, 1995.
2. A V Bronnikov and D Killian, '3D tomography of turbine blades', Proceedings of International Symposium on Computerized Tomography for Industrial Applications and Image Processing in Radiology, Berlin, Germany, pp 173-180, March 1999.
3. F Losano, *et al*, 'Computed tomography in the automotive field: development of a new engine head case study', Proceedings of International Symposium on Computerized Tomography for Industrial Applications and Image Processing in Radiology, Berlin, Germany, pp 65-74, March 1999.
4. A Flisch, *et al*, 'Industrial computed tomography in reverse engineering applications', Proceedings of International Symposium on Computerized Tomography for Industrial Applications and Image Processing in Radiology, Berlin, Germany, pp 45-54, March 1999.
5. M Simon and C Sauerwein, 'Quality control of light metal castings by 3D computed tomography', Proceedings of 15th World Conference on Nondestructive Testing, Rome, October 2000.
6. L A Feldkamp, L C Davis and J W Kress, 'Practical cone-beam algorithm', J. Opt. Soc. Am. A, Vol 1, No 6, pp 612-619, June 1984.
7. G T Gullberg, C R Crawford and B M W Tsui, 'Reconstruction algorithm for fan beam with a displaced center-of-rotation', IEEE Transactions on Medical Imaging, Vol MI-5, No 1, pp 23-29, March 1986.

DOI: 10.1784/insi.2008.50.1.22

Adaptive filtering for image enhancement and noise reduction in computed tomography images

N Saxena, G L Baheti, D K Tripathi, K C Songara, L R Meghwal and V L Meena

Submitted 2 April 2007
Accepted 9 July 2007

Computed Tomography (CT) is being increasingly utilised as a powerful tool for advanced Non-Destructive Testing and Evaluation (NDT&E) applications. CT images reconstructed from the attenuation datasets, particularly in the first and second generation CT systems, are prone to various noise and artefacts; hence, a need exists to explore post-filtering options with an aim of image enhancement and noise reduction. However, this has to be achieved in such a way that the basic features and edges are not lost in the processing.

In the present work, 2-D adaptive filtering has been applied and studied in comparison with conventional non-adaptive centred averaging filtering for various CT images. Adaptive filters have been implemented by computing the central pixel value using neighbourhood centred averaging and subsequently applying the adaptive correction on each pixel using the local variance and overall noise variance estimates. The paper highlights the results of non-adaptive and adaptive filtering on various CT images. Adaptive filtering has been found to provide excellent results for noise reduction and image enhancement of CT images, without losing information of edges, boundary and feature details.

Keywords: Adaptive filtering, image processing, tomography imaging.

1. Introduction

Computed Tomography (CT) is an advanced non-destructive testing and evaluation technique which provides complete cross-sectional visualisation[1,2]. In CT, the object to be scanned is illuminated by X/gamma radiation beam and attenuation measurements are made at multiple points through the object for multiple projection angles. These measurements are stored and fed to image reconstruction algorithms to generate images representing 2-D slices of object planes which reveal complete cross-sectional details. The power of CT lies in its ability to unfold absorption data taken from multiple angles and producing maps of the local absorption at all points inside the scanned object thereby providing complete object visualisation. The fundamental equation governing the attenuation of nuclear radiation as it passes through any material is as follows:

$$I = I_0 e^{-\mu x}$$

where: I_0 is the incident radiation intensity,
μ is the linear attenuation coefficient,
x is the material thickness encountered, and
I is the output intensity.

Nisheet Saxena, G L Baheti, D K Tripathi, K C Songara, L R Meghwal and V L Meena are in the Nuclear Radiation Management & Applications Division, Defence Laboratory, Jodhpur – 342011, India. Tel: 91-291-2510641; Fax: 91-291-2511191; E-mail: nisheets@yahoo.com

The measurement of output radiation intensity across different points through the object illuminated by radiation source, at multiple angles, forms the basis for tomographic reconstructions.

Defence Laboratory, Jodhpur has developed single and multi-detector CT systems for defence applications[3,4]. CT images reconstructed from the attenuation data are prone to noise and features vary tremendously in industrial components; hence, a need exists to explore post-filtering options with an aim of image enhancement and noise reduction. However, this has to be achieved in such a way that the basic features and edges are not lost in the processing.

2. Present study

In the present study, neighbourhood averaging 2-D filters have been implemented using 'C' and 'Tcl-Tk' under Linux Environment and their effects have been studied on CT images. The adaptive variant of the filter has been implemented using local variance and noise variance estimates for the images. All these 2-D filters have been implemented with options of two kernel sizes *ie* 3×3 and 5×5 matrices.

3. Theoretical review

3.1 Sources of noise

The most common source of noise in typical first and second generation CT systems is the poor counting statistics in nuclear detections because of the constraints of low data acquisition times and a need to scan the object in a faster mode. Noisy images can also occur due to instability in radiation source or detector during the scanning.

Noise thus, gets introduced into a CT image in many ways, starting with the X/gamma nuclear counting statistics, detector performance, motion instabilities, storage efficiencies, scanning parameters, and reconstruction algorithm constraints.

The images may have some defects that may be present due to imperfect detectors, inadequate or non-uniform illumination. The reduction of noise without degradation of the underlying image has attracted much attention in the past. However, whilst many 'structure preserving' filters have achieved some degree of success at preserving one dimensional image structure, very few have successfully preserved two dimensional image brightness structure, such as corners, edges and junctions[5].

3.2 Conventional linear filtering

The simplest way to accomplish a conventional linear filtering is by neighbourhood averaging, *ie* replacing each pixel with the average of itself and its neighbours. Different kernel weightages and sizes can be utilised. Figures 1 and 2 show typical values for 3×3 and 5×5 kernels based on centred averaging which have been utilised in the present study. The boundaries have been excluded for processing operations.